Balanced Binocular Inputs Support Superior Stereopsis

Xi Wang,[1–3] Alex S. Baldwin,[3] and Robert F. Hess[3]

[1]Department of Ophthalmology, West China Hospital, Sichuan University, Chengdu, Sichuan, China
[2]Laboratory of Optometry and Vision Sciences, West China Hospital, Sichuan University, Chengdu, Sichuan, China
[3]McGill Vision Research Unit, Department of Ophthalmology & Visual Sciences, McGill University, Montreal, Quebec, Canada

Correspondence: Xi Wang, Department of Ophthalmology, West China Hospital, Sichuan University, 37 Guoxue Xiang, Chengdu, Sichuan 610041, China; xiwangoph@126.com.

Received: March 5, 2021
Accepted: July 26, 2021
Published: September 13, 2021

Citation: Wang X, Baldwin AS, Hess RF. Balanced binocular inputs support superior stereopsis. *Invest Ophthalmol Vis Sci.* 2021;62(12):10. https://doi.org/10.1167/iovs.62.12.10

Purpose. Our visual system compares the inputs received from the two eyes to estimate the relative depths of features in the retinal image. We investigated how an imbalance in the strength of the input received from the two eyes affects stereopsis. We also explored the level of agreement between different measurements of sensory eye imbalance.

Methods. We measured the sensory eye imbalance and stereoacuity of 30 normally sighted participants. We made our measurements using a modified amblyoscope. The sensory eye imbalance was assessed through three methods: the difference between monocular contrast thresholds, the difference in dichoptic masking weight, and the contribution of each eye to a fused binocular percept. We referred them as the "threshold imbalance," "masking imbalance," and "fusion imbalance," respectively. The stereoacuity threshold was measured by having subjects discriminate which of four circles were displaced in depth. All of our tests were performed using stimuli of the same spatial frequency (2.5 cycles/degree).

Results. We found a relationship between stereoacuity and sensory eye imbalance. However, this was only the case for fusion imbalance measurement ($\rho = 0.52$; $P = 0.003$). Neither the threshold imbalance nor the masking imbalance was significantly correlated with stereoacuity. We also found the threshold imbalance was correlated with both the fusion and masking imbalances ($r = 0.46$, $P = 0.011$ and $r = 0.49$, $P = 0.005$, respectively). However, a nonsignificant correlation was found between the fusion and masking imbalances.

Conclusions. Our findings suggest that there exist multiple types of sensory eye dominance that can be assessed by different tasks. We find only imbalances in dominance that result in biases to fused percepts are correlated with stereoacuity.

Keywords: sensory eye imbalance, stereopsis, binocular function

In binocular vision, we integrate monocular visual information into a combined percept of the surrounding world. Along with the composite image of the two eye's inputs, the visual system is also able to use the differences between the two eyes to calculate depth. This "stereopsis" makes use of the binocular disparity derived from the objects at different depths projecting to slightly different locations on the retinas in the two eyes. It is interesting that, even in subjects with healthy eyes, we find a wide variability in stereoacuity in the population.[1–5] In a recent study, we showed that stereoacuity is broadly distributed. It extends over more than a hundred-fold range across the population. The distribution of stereoacuity did not seem to be unimodal. Instead, our results suggested that the population of normally sighted individuals contains a large subgroup (approximately one-third) who have markedly poorer stereo than the remaining two-thirds.[6]

Stereopsis involves both fusion and suppression processes. The fusion process constructs a stereo percept by integrating the inputs from similar features in the images seen by the two eyes. At the same time, the dissimilar inputs from one eye are suppressed to promote a single binocular percept. The inputs from two eyes may not be balanced equally. One of the eyes may make a stronger contribution to the binocular percept.[7] Both imbalanced temporal and spatial visual inputs could affect stereopsis. Previous studies have reported that interocular delay is associated with stereo perception, like the Pulfrich phenomenon.[8–10] In addition, the extent of the ocular dominance imbalance from the spatial visual inputs of the two eyes varies in the population.[11–14] This sensory eye imbalance may also affect stereopsis. In an extreme example, subjects with amblyopia have both a strong imbalance in their eye dominance and also typically exhibit poor (or no) stereopsis.[15–17] However, whether the sensory eye imbalance limits stereoacuity in subjects without amblyopia is controversial.

The relationship between sensory eye imbalance and stereopsis in the normally sighted population has been explored in recent studies. Xu et al.[18] measured the sensory eye balance and stereoacuity by using binocular rivalry stimuli and a random dot stereogram. They found observers with large sensory eye imbalance had poor stereoacuity. Similar results were reported by Cooper and Mendola,[19] who used both binocular rivalry and dichoptic masking to measure the

degree of imbalance, and by Han et al.,[20] who used binocular rivalry and binocular phase combination. These studies measured stereoacuity with spatially broadband random dot stimuli, while using lower frequency gratings for their measure of sensory eye balance. However, Wang et al.[14] measured sensory eye balance and stereoacuity at the same low spatial frequency using a binocular phase combination task. They found that the two measurements were not correlated significantly. Not only did these studies differ in the relative spatial frequency used to assess sensory eye balance and stereoacuity, but also in the absolute spatial frequency. Wang et al. used a low-spatial frequency stimulus (0.3 c/deg) to assess stereoacuity, whereas Xu et al.[18] and Cooper and Mendola[19] used a moderate spatial frequency (ie, 2.5 c/deg).

In this study, we are similarly interested in how sensory eye imbalance affects stereoacuity in the population with normal or corrected-to-normal visual acuity. We assessed the sensory eye imbalance by measuring the difference between monocular contrast thresholds, the difference in dichoptic masking weight, and the contribution of each eye to fusion binocular vision by using a binocular orientation combination task.[21] All of these measurements were evaluated at the same spatial frequency (2.5 c/deg). Because stereoacuity could vary with spatial frequency of the testing stimuli,[22,23] we measured stereoacuity at the same spatial frequency. We set out to address two questions: (1) Does stereoacuity at a moderate spatial frequency (2.5 c/deg) vary with the magnitude of sensory eye imbalance when both are measured at that same spatial scale? That is to say, does a better balance between the two eyes mean better stereo? (2) How are the different measurements of sensory eye imbalance related to each other when made at the same moderate spatial frequency (2.5 c/deg)?

Methods

Participants

Thirty adults (average age, 31 years old; range, 20–69 years old) with normal or corrected-to-normal visual acuity participated in this study. All participants reported no history of binocular dysfunction or ocular surgery. Subjects performed the experiment with their best optical correction if needed. This study followed the tenets of Declaration of Helsinki, and was approved by Ethics Review Board of the McGill University Health Center. Written informed consent was obtained from all participants before data collection.

Equipment

Supplementary Figure S1 shows our experimental setup. An Apple MacBook Pro running MATLAB (MathWorks, Natick, MA) with Psychtoolbox 3.0.9 extension was used to generate the stimuli. The stimuli were displayed on a pair of gamma-corrected screens (refresh rate 75 Hz, resolution 800 × 600 pixels, mean luminance 87 cd/m^2). We wrote a customized bit-stealing algorithm (after Tyler[24]) to simultaneously increase the bit depth, linearize the luminance response of the screens, and make the two screens behave equivalently to each other. The screens were installed in a modified amblyoscope (Clement Clarke, Made in England), also referred to as a synoptophore. A typical amblyoscope uses an optical system to allow images to be aligned when presented dichoptically to the two eyes of a patient. The mechanism of the amblyoscope allows for 90° of movement per eye. The images used for the alignment are traditionally a pair of slides. Our modified amblyoscope replaces the standard slide presentation with the two LCD screens described elsewhere in this article. This setup allows us to present computer-rendered stimuli dichoptically with control over their alignment. The participants viewed the stimuli presented separately to each eye through the eyepieces of the modified amblyoscope. The effective viewing distance was 17.5 cm. At this distance, there were 28 pixels on the screen for each degree of visual angle.

Stimuli and Procedure

General Procedure. Subjects completed a battery of tasks using the modified amblyoscope. This process began with an alignment of the images seen by the two eyes. The standard alignment slides typically used in the amblyoscope were reinserted for this step. Subjects only used a single degree of freedom of the equipment for their alignment. The equipment was adjusted to a large horizontal angle, and then the subject decreased that angle until they comfortably saw a fused image. These adjustments were repeated to ensure they resulted in a stable value. The slides were removed, and subjects then completed a series of psychophysical tasks.

Testing began with a modified version of the Worth 4 Dot test. The right eye was presented with two red dots placed vertically one above the other. The left eye was presented with three green dots forming a V-shaped triangle with its bottom point aligned with the lower red dot presented to the other eye. The two other green dots flanked the center point between the upper and lower red dot. In normal binocular vision, this image is seen as a diamond array of four dots. The upper dot is red, the left and right dots are green, and the bottom dot is bistable and the percept alternates between red and green. Other responses may indicate anomalies of binocular vision. All the subjects exhibited normal fusion.

After presenting the dot stimuli to the patient, we asked whether the bottom dot was seen as a single dot or whether two dots were visible. All subjects saw a single bottom dot without further adjusting the amblyoscope. This indicated that the initial alignment was successful.

Monocular Contrast Detection Threshold. Contrast detection thresholds were measured in each eye. The stimuli to be detected were sinusoidal gratings (Fig. 1A). They had a spatial frequency of 2.5 c/deg. The method was a two-alternative forced-choice (2AFC) task where subjects were asked to identify the orientation of the presented grating. The gratings could be presented with the bars sloping at either −45° or +45° (left or right oblique). The spatial extent of the grating was limited by a circular raised-cosine envelope with the plateau of 3° of visual angle and cosine half-period of 0.2°. The temporal properties of the presentation were also controlled by a raised cosine function. The contrast first increased from zero to the nominal contrast according to the shape of a half-period of a cosine function over 240 ms. There was then a 240 ms plateau where the stimulus remained at its nominal contrast. Then, the contrast decreased from the nominal contrast to zero, mirroring the initial increasing ramp (again over 240 ms). Therefore, the duration for which the stimulus was presented at more than half of its nominal contrast (full width at half magnitude) was 480 ms.

Grating contrast was calculated as root mean square contrast before applying the spatial envelope. This is simply the standard deviation of the pixel values when the mean of

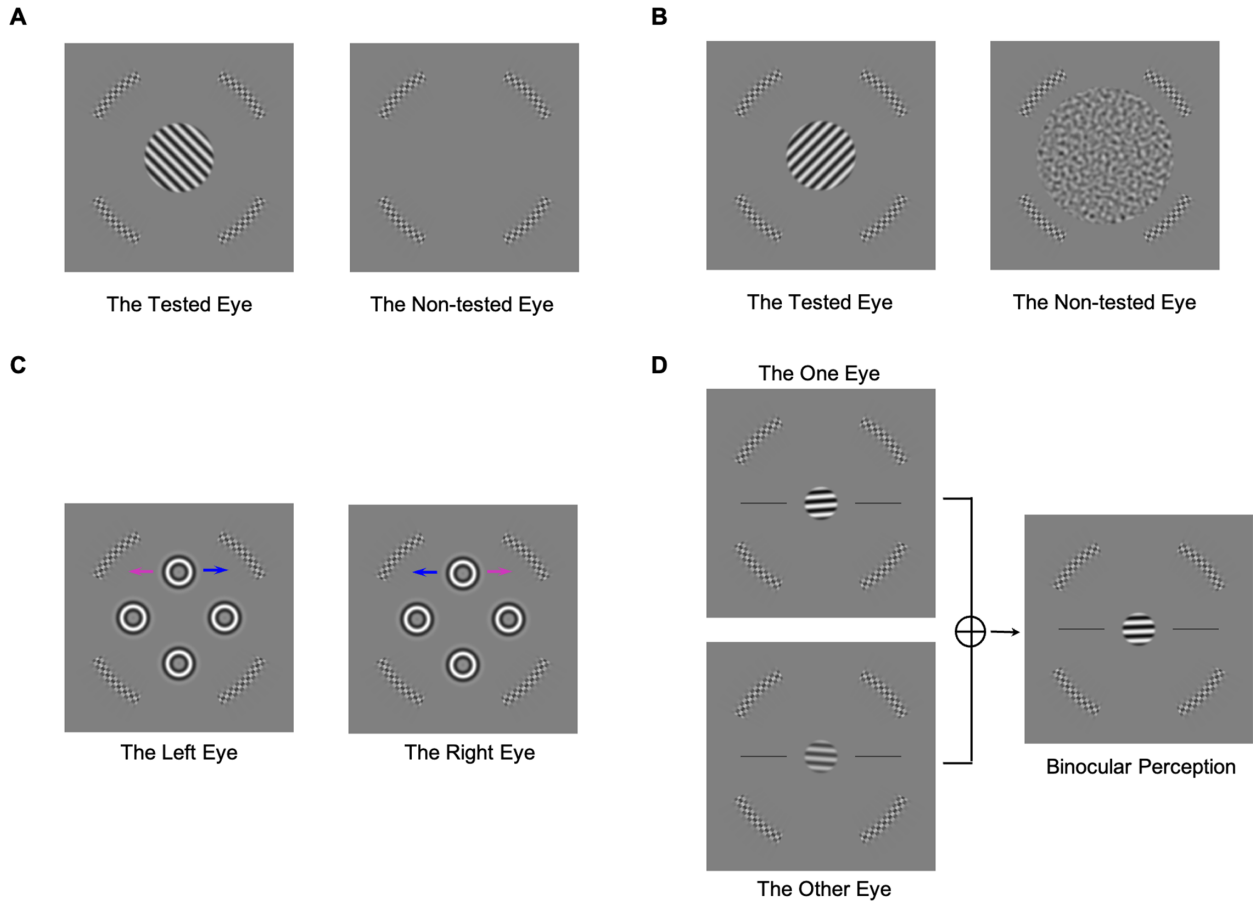

Figure 1. Sample stimuli of the four tasks in this study. (**A**) Monocular contrast detection threshold test. (**B**) Dichoptic masking test. (**C**) Stereo threshold test. The arrows indicate the direction of horizontal offset in each eye (blue arrows for inward or pink arrows for outward). (**D**) Binocular orientation combination test.

the stimulus is zero and +1 and −1 are the maximum and minimum presentable luminances. For any stimulus there is a 1:1 linear relationship between the root mean square contrast and the Michelson contrast. We present stimulus contrast in decibel logarithmic units, calculated as

$$c_{\mathrm{dB}} = 20 \times \log_{10}(c_{\mathrm{RMS}}).$$

We used a 2AFC method to obtain thresholds for detecting a grating presented to one eye. Throughout the experiment, a binocular frame was presented around the stimuli to help the participants maintain their convergence. The eye being tested was randomly selected on each trial. The target grating was presented only to the tested eye. Subjects then pressed one of two buttons to indicate the orientation of the target grating (−45° or +45°). They were given an audio feedback based on whether they were correct. Target grating contrast was controlled by a pair of staircases[25] (one for each eye). Each of them had a three-down–one-up rule and a 3-dB step size (therefore converging the staircase sampling at the 79% correct point[26]). The initial grating contrast was −12 dB. The 2 staircases were randomly interleaved and terminated after 9 reversals or 120 trials for each (whichever was reached first). Subjects completed two repetitions of this test. Data from the two repetitions were combined. Psychometric functions were fit to the combined data for each eye to obtain the monocular thresholds (see the Data Analysis section).

Dichoptic Masking Thresholds. After measuring contrast detection thresholds, we next measured the strength of dichoptic masking. On each trial, the tested eye was presented with a sinusoidal grating similar to that used in the previous test. The other eye was presented with a patch of contrast-modulated noise (Fig. 1B). The noise was generated by filtering white noise with an isotropic log-Gabor filter. The peak spatial frequency of the noise was the same as for the grating (2.5 c/deg). The spatial frequency bandwidth of the noise was 1.4 octaves. The spatial extent of the noise masks was controlled by a circular raised-cosine envelope. The width of the plateau was 6° and cosine half-period was 0.2°. We used the same temporal envelope as used for the gratings to control the presentation duration of the noise.

We used a 2AFC method in combination with an adaptive staircase procedure to measure dichoptic masking. However, in this test we fixed the contrast of the grating stimuli. In each eye, they were presented at a fixed level above that eye's contrast detection threshold. This was the monocular contrast detection threshold plus 9 dB. We then controlled the contrast of the noise presented to the other eye using our staircases (one staircase for each eye). The staircases used a three-down–one-up rule with a 3-dB step size. The direction of travel was reversed compared to the staircase in the

Investigative Ophthalmology & Visual Science

previous test (as increasing the noise contrast makes the task harder). The initial noise contrast was set at −36 dB. After each trial, subjects were asked to indicate the orientation of the grating. They were given an audio feedback based on whether they were correct. Subjects completed two repetitions of the test. Data were combined across the repetitions and the psychometric functions were fit to find threshold levels of the dichoptic mask required to have a criterion effect on detection performance for suprathreshold targets.

Stereo Thresholds. We measured stereo thresholds using a digital stereo task. The stimuli were four identical spatially bandpass circles (spatial frequency 2.5 c/deg, circle diameters 1°). These were generated with a cross-section based on the fourth-order derivative of the Gaussian function. This method is similar to that used to generate radial frequency patterns.[27] The four circles were arranged into a diamond shape (four locations: top, bottom, left, and right). Each circle was placed at an eccentricity of roughly 2° from the center of the display. Each circle was presented binocularly; however, one of the four was presented with a horizontal disparity. This disparity was achieved by adding equal and opposite horizontal offsets to the positions of a particular circle shown to each eye. The direction of horizontal offset in each eye (inward or outward) determined whether the binocular perception of the circle would have a crossed or uncrossed disparity (Fig. 1C). These offsets will break-up the diamond shape formed by the four circles. To prevent this being used as a cue, all of the horizontal and vertical positions of the circles were slightly randomized (with the same random offsets being used in the two eyes). The amount of this randomization was equal to the one-half of the disparity shift in each trial.

We conducted a psychophysical test using a four-alternative-force choice to obtain the stereo thresholds. Subjects indicated which circle had depth by pressing one of the four keys. They were given an audio feedback based on their performance. The direction of the target disparity (crossed or uncrossed) and the location of the target circle were randomly selected on each trial. Two staircases were used to control the disparity. Each of them had a two-down–one-up rule with the step size set to a ratio of $\sqrt{2}$. The initial disparity was 512 arc sec. The two staircases were randomly interleaved and terminated after 9 reversals or 30 trials for each (whichever was reached first). Subjects completed two repetitions of the measurement. Data were combined across the repetitions and the psychometric functions were fit to the combined data to find stereo thresholds.

Binocular Eye Balance. Finally, we measured the contribution of each eye to fused binocular vision. We used a binocular orientation combination task as described by Wang et al.[21] As illustrated in Figure 1D, the stimuli were a pair of dichoptically presented tilted gratings (2.5 c/deg). The two gratings had an equal and opposite tilt of 4°. The gratings had a spatial envelope with a plateau of 1.4° and a cosine half-period of 0.2°, and the same temporal envelope as described elsewhere in this article. They were accompanied by two black reference horizontal lines and surrounded by the circular frame. The base contrast of the gratings was 45%. We measured the binocular orientation combination at seven interocular contrast ratios (1/4, 1/2, $1/\sqrt{2}$, 1, $\sqrt{2}/1$, 2, and 4). For each of these ratios, the contrast in one eye was increased and the contrast in the other eye was decreased to achieve that specific ratio. There were 20 repetitions for each ratio. In each trial, the interocular ratio was chosen randomly. Binocular presentation of these two gratings produced one fused grating percept. The relative strength of the stimulus seen by each eye determined the weight of its contribution to the binocular percept. Subjects then were asked to answer which side of this grating (left or right) was tilted up by pressing one of the two buttons. After data collection, psychometric functions were fit to find the balance point of the two eyes.

Data Analysis

We obtained the monocular contrast detection thresholds, dichoptic masking thresholds, and stereo thresholds by fitting logistic psychometric functions using Palamedes.[28] In all cases, the lapse rate was fixed at 1% for fitting. The thresholds for the 2AFC and four-alternative-force choice data were calculated at a proportion correct of 75.0% and 62.5%, respectively. We used parametric bootstrapping routines to obtain bootstrapped estimates of standard error and 95% confidence intervals (1000 samples).

We obtained interocular suppression weights by fitting our data with the two-stage model of contrast gain control based on that described by Meese et al.[29] For the case where targets are presented to the left eye, the response at the first stage is given by:

$$resp_L = \frac{(g_L \times C_L)^m}{1 + g_L \times C_L + \omega_R \times g_R \times C_R}, \quad (1)$$

where C_L and C_R are the contrasts of the target in the left eye and the mask in the right eye, respectively. The three fitted parameters are the gain in the left and right eyes (g_L and g_R) and the interocular masking weight from the right eye w_R. The exponent m is set at 1.3 based on previous results.[30] The target is only presented to one eye at a time, so for targets presented in the left eye the second stage is given by

$$resp = \frac{resp_L^p}{1 + resp_L^q}, \quad (2)$$

where p, and q are fixed at $p = 8$, and $q = 6.6$ based on previous results. Therefore, accounting for left and right eye target conditions requires four fitted model parameters: g_L, g_R, w_L, and w_R. It is worth noting that the construction of Equation 1 means that the masking weight parameters for each eye have an effect that is separate from the input gain parameters. Any imbalances found in masking weight are additional to the effects of any imbalances in input gain. Assuming a constant internal noise variance, predicting thresholds requires simply solving for some criterion value of $resp$ (we chose to solve for a value of $resp = 1$). We fit this model in MATLAB using the fminsearch function to minimize the root mean square error between the thresholds predicted by the model and the empirical data.

To obtain the balance point of each subject, we fitted the proportion of trials in which they reported that the left side of the grating tilted up by using a logistic function. The estimated midpoint of the logistic function defines the point of subjective equality, which indicates the balance point where the two eyes were balanced in binocular combination. For this analysis, the lapse rate of 1% affected both the upper and lower asymptotes (gamma and lambda parameters) of the psychometric function. The estimated points of subjective equality were derived from 1000 parametric bootstrapped samples.

Investigative Ophthalmology & Visual Science

Results

Stereoacuity, monocular contrast thresholds, and monocular dichoptic masking thresholds are respectively presented in Figures 2A, C, E. Interocular differences in contrast threshold and interocular differences in masking weight were obtained by the monocular contrast thresholds and monocular dichoptic masking thresholds. The mean absolute interocular difference in contrast thresholds was 2.9 ± 0.5 dB (mean ± standard error; 95% confidence interval [CI], 2.0–3.9). The mean absolute interocular difference in masking weight was 9.5 ± 1.1 dB (95% CI, 7.2–11.8). The mean stereoacuity was 6.1 ± 0.2 $\log_2$ (arc sec) (95% CI, 5.7–6.4). Inverting the log-transformation gives an average threshold of 69 arc sec. The mean absolute

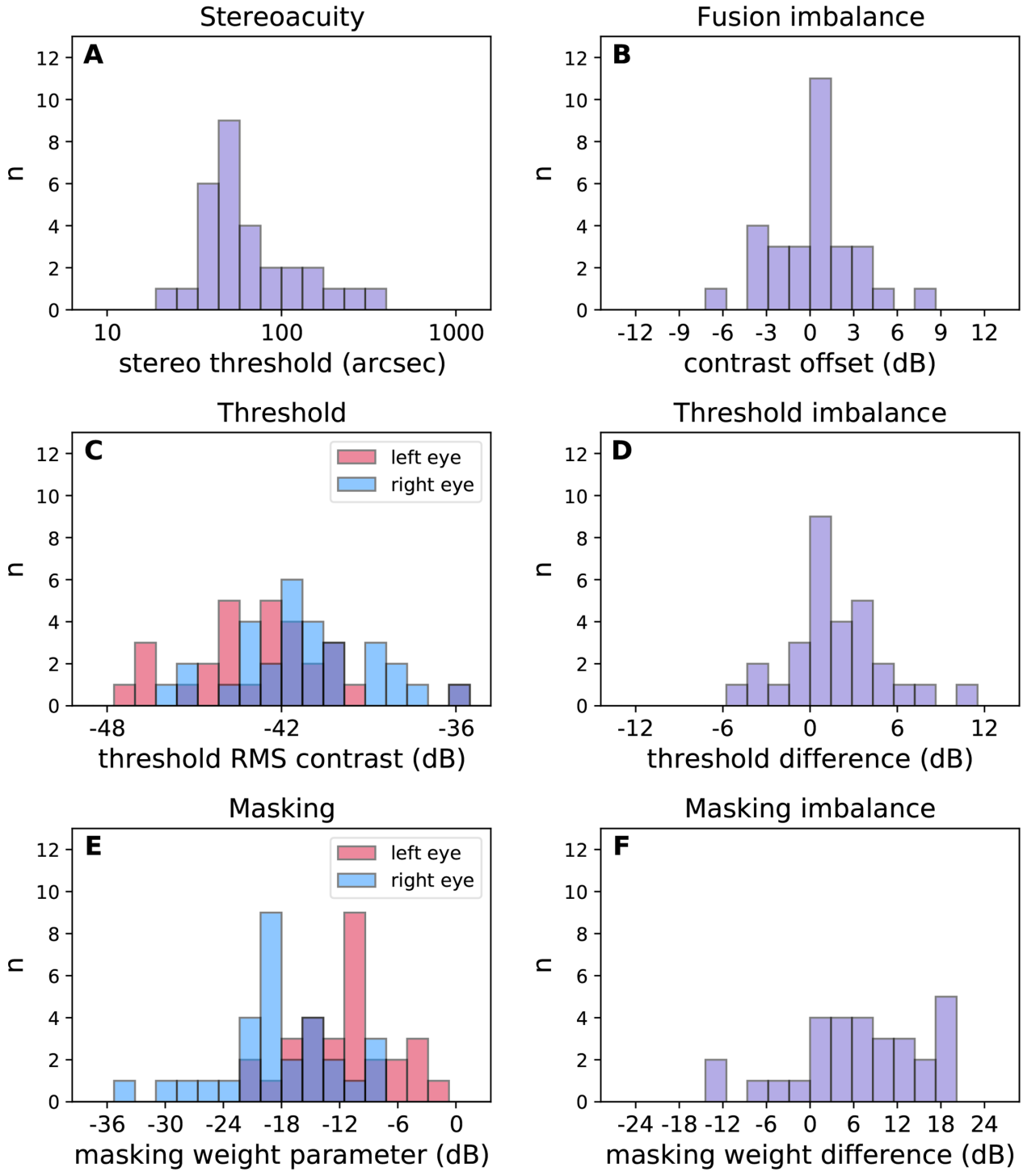

Figure 2. Histograms showing the distribution of stereoacuity (**A**), monocular contrast thresholds (**C**), and monocular dichoptic masking thresholds (**E**) in all subjects. (**B**, **D**, **F**) Plot distribution of fusion imbalance, threshold imbalance, and masking imbalance respectively. (Negative value along the *x*-axis of each graph represent the amount of right eye sensory eye dominance.) RMS, root mean square.

Investigative Ophthalmology & Visual Science

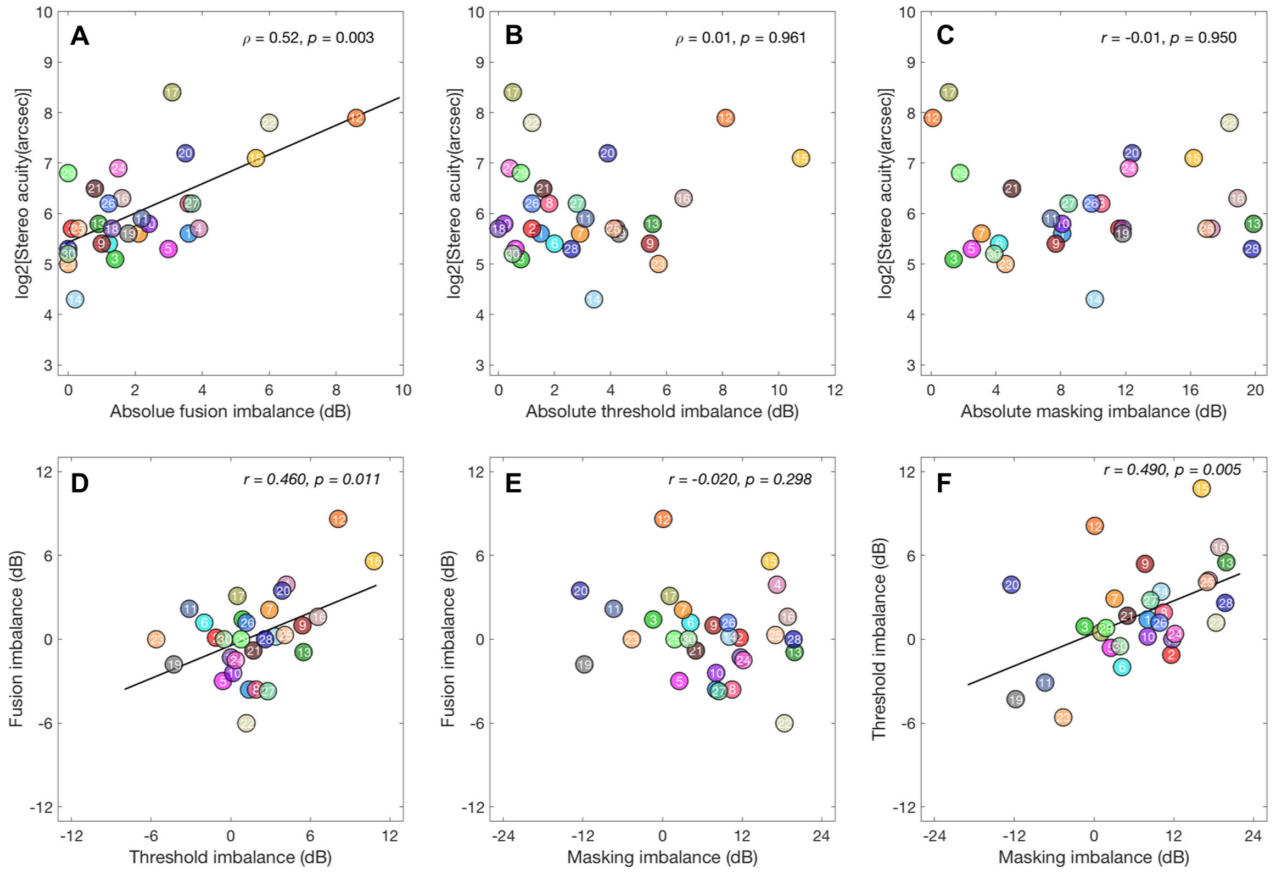

Figure 3. Correlations between measures of binocular functions. (**A–C**) Stereoacuity versus sensory eye imbalances (absolute fusion imbalance, absolute threshold imbalance, and absolute masking imbalance, respectively). (**D**) Fusion imbalance versus threshold imbalance. (**E**) Fusion imbalance versus masking threshold. (**F**) Threshold imbalance versus masking threshold. The same numbered circle marker indicates the same subject.

balance point was 2.2 ± 0.4 dB (95% CI, 1.4–2.9). We also display the distributions of the measures of binocular function with signed value in all subjects.

For each of those measures, we refer to them as a type of sensory eye imbalance. For the binocular fusion task with the oriented gratings, the value of the balance point for when the two eyes contribute equally to the percept is termed the "fusion imbalance." In the threshold task, the difference in threshold between the two eyes is termed the "threshold imbalance." With the dichoptic mask, the difference in masking weight between the two eyes is termed the "masking imbalance." The results of those sensory eye imbalance are presented in Figures 2B, D, F. Negative value along the *x*-axis of each graph represent the amount of right eye sensory eye dominance.

Figures 3A, B, C each plot the subject's stereoacuity as a function of sensory eye imbalance. We performed a Shapiro–Wilk test on the normality of the data distribution. The absolute fusion imbalance and absolute threshold imbalance were not normally distributed ($P = 0.002$ and $P = 0.004$, respectively). The Spearman's ρ correlation test and Pearson's r correlation test were used to analyze as appropriate. We found a significant correlation between stereoacuity and the absolute fusion imbalance (Fig. 3A; $\rho = 0.52$; 95% CI, 0.17–0.76; $P = 0.003$), suggesting that the subjects with well-balanced contributions to binocular vision from the two eyes have better stereopsis. However, we found no significant correlation between stereoacuity and the absolute threshold or masking imbalances (Fig. 3B; $\rho = 0.01$; 95% CI, −0.39 to 0.38; $P = 0.961$; Fig. 3C, $r = -0.01$; 95% CI, −0.38 to 0.48; $P = 0.950$). This finding suggests that imbalances in performance at threshold or the effectiveness of dichoptic masking do not predict stereoacuity.

In addition, we examined the correlation between the different measures of sensory eye imbalance. We found significant (but moderate) correlations between fusion imbalance and threshold imbalance (Fig. 3D; $r = 0.46$; 95% CI, 0.05 to 0.7; $P = 0.011$), and between threshold imbalance and masking imbalance (Fig. 3F; $r = 0.49$; 95% CI, 0.12 to 0.79; $P = 0.005$). These accounted for 21% and 24% of the variance, respectively. We found no significant correlation between fusion imbalance and masking imbalance (Fig. 3E; $r = -0.20$; 95% CI, −0.5 to 0.17; $P = 0.298$).

Discussion

In this study, we assessed stereoacuity and sensory eye imbalance in subjects with normal healthy vision, and examined the relationships between these measures. The average stereoacuity was 69 arc sec. Stereoacuity was distributed over a broad range (Fig. 2A, Fig. 3A), which is similar to previous studies.[1,3,6] We also showed that the inputs from the two eyes are not perfect balanced in subjects with

Investigative Ophthalmology & Visual Science

otherwise normal vision. The extent of the imbalance also varied over a significant range (Fig. 2, Fig. 3). Our results showed that stereoacuity significantly correlated with fusion imbalance, but not with absolute contrast threshold or contrast masking imbalance. In addition, we found some correlations between these three measures of sensory eye imbalance. There was a moderate correlation between the fusion and threshold imbalances; however, we did not find a correlation between fusion and masking imbalances. The construction of Equation 1 gives us a measure of masking imbalance that factors out the effects of any imbalances in input sensitivity to the two eyes. Even with these effects factored out, however, we found a moderate correlation between threshold and masking imbalances. Because the threshold imbalance was correlated with both the fusion and masking imbalances, it is perhaps a little surprising that the fusion and masking imbalances were not significantly correlated with each other. This finding can be explained by the significant correlations we found not being very strong. It is possible that the subset of data points driving the correlation between fusion and threshold imbalances are not the same as the subset of data points driving the correlation between threshold and masking imbalances.

Our results show a relationship between stereoacuity and sensory eye balance, but only when balance is assessed with a task that measures fusion for suprathreshold stimulation. We do not find a relationship between stereoacuity and measures of eye balance at threshold. This finding is in agreement with previous studies that found stereoacuity was significantly correlated with sensory eye balance.[18–20] However, our study has the advantage of measuring eye balance and stereoacuity using stimuli of the same spatial frequency. Both stereoacuity[22,23] and sensory eye balance[21] are known to depend on stimulus spatial frequency and so it is essential to use targets of the same spatial frequency for their comparison. However, our results are in disagreement with a previous study that used the same spatial frequency to make these two measurements. Wang et al.[14] assessed sensory eye balance and stereoacuity in a relatively large sample (142 adults) by using a binocular phase combination task. They found that stereopsis was not correlated significantly with sensory eye balance. However, a possible explanation was that their spatial frequency was relatively low (0.3 c/deg). Our results suggest that their conclusions do not apply to higher spatial frequencies.

The spatial frequency used in our study was comparable with that used in previous studies that did find a relationship between sensory eye balance and stereoacuity.[18–20] Although the relatively moderate sample size of our study may decrease the statistical power, we still found a strong correlation between stereoacuity and the sensory eye balance (Fig. 3A), suggesting that the subjects with well-balanced contributions to binocular vision from the two eyes have better stereopsis (at least when assessed by a task that measure's the contribution from the two eyes to suprathreshold perception). We hypothesize that this relationship may be dependent on spatial frequency.

The subjects in this study ranged in age from 20 to 69 years old; however, we had not set out to study any effects of age and so did not analyze this aspect of our data (because we would have lacked statistical power). It would be useful in subsequent studies to set out with a view to performing a specific analysis on this dimension of interest, by recruiting a larger number of subjects across a range of ages. This would allow for a further evaluation of the relationship between stereoacuity and the sensory eye balance across the lifespan.

Acknowledgments

Supported by the Canadian Institutes of Health Research Grants CCI-125686 and Post-Doctor Research Project, West China Hospital, Sichuan University (2020HXBH167).

Disclosure: **X. Wang,** None; **A.S. Baldwin,** (P) PCT Patent Application (CA2020050051) titled "System and Method for Digital Measurement of Stereo Vision." This invention has been commercially licensed by McGill University to Novartis International AG. Development of this invention has been supported (separately and independently from this study) by grants, personal fees, and nonfinancial support from Novartis International AG under a research agreement with the Research Institute of the McGill University Health Centre; **R.F. Hess,** (P) PCT Patent Application (CA2020050051) titled "System and Method for Digital Measurement of Stereo Vision." This invention has been commercially licensed by McGill University to Novartis International AG. Development of this invention has been supported (separately and independently from this study) by grants, personal fees, and nonfinancial support from Novartis International AG under a research agreement with the Research Institute of the McGill University Health Centre

References

1. Richards W. Stereopsis and stereoblindness. *Exp Brain Res.* 1970;10(4):380–388.
2. Zaroff CM, Knutelska M, Frumkes TE. Variation in stereoacuity: normative description, fixation disparity, and the roles of aging and gender. *Invest Ophthalmol Vis Sci.* 2003;44(2):891–900.
3. Bosten JM, Goodbourn PT, Lawrance-Owen AJ, et al. A population study of binocular function. *Vision Res.* 2015;110(Pt A):34–50.
4. Tittes J, Baldwin AS, Hess RF, et al. Assessment of stereovision with digital testing in adults and children with normal and impaired binocularity. *Vision Res.* 2019;164:69–82.
5. Alarcon Carrillo S, Baldwin AS, Hess RF. Factors limiting sensitivity to binocular disparity in human vision: evidence from a noise-masking approach. *J Vis.* 2020;20(3):9.
6. Hess RF, To L, Zhou J, Wang G, Cooperstock JR. Stereo vision: the haves and have-nots. *Iperception.* 2015;6(3):2041669515593028.
7. Cumming BG, DeAngelis GC. The physiology of stereopsis. *Annu Rev Neurosci.* 2001;24:203–238.
8. Plainis S, Petratou D, Giannakopoulou T, et al. Small-aperture monovision and the Pulfrich experience: absence of neural adaptation effects. *PLoS One.* 2013;8(10):e75987.
9. Reynaud A, Hess RF. Interocular contrast difference drives illusory 3D percept. *Sci Rep.* 2017;7(1):5587.
10. Atchison DA, Lee J, Lu J, et al. Effects of simulated anisometropia and aniseikonia on stereopsis. *Ophthalmic Physiol Opt.* 2020;40(3):323–332.
11. Ooi TL, He ZJ. Sensory eye dominance. *Optometry.* 2001;72(3):168–178.
12. Li J, Lam CS, Yu M, et al. Quantifying sensory eye dominance in the normal visual system: a new technique and insights into variation across traditional tests. *Invest Ophthalmol Vis Sci.* 2010;51(12):6875–6881.
13. Jiang F, Chen Z, Bi H, et al. Association between ocular sensory dominance and refractive error asymmetry. *PLoS One.* 2015;10(8):e0136222.
14. Wang Y, Cui L, He Z, et al. On the relationship between sensory eye dominance and stereopsis in the

normal-sighted adult population: normative data. *Front Hum Neurosci.* 2018;12:357.
15. Li J, Thompson B, Lam CS, et al. The role of suppression in amblyopia. *Invest Ophthalmol Vis Sci.* 2011;52(7):4169–4176.
16. Kwon M, Lu ZL, Miller A, et al. Assessing binocular interaction in amblyopia and its clinical feasibility. *PLoS One.* 2014;9(6):e100156.
17. Webber AL, Wood JM, Thompson B, Birch EE. From suppression to stereoacuity: a composite binocular function score for clinical research. *Ophthalmic Physiol Opt.* 2019;39(1):53–62.
18. Xu JP, He ZJ, Ooi TL. A binocular perimetry study of the causes and implications of sensory eye dominance. *Vision Res.* 2011;51(23-24):2386–2397.
19. Cooper PR, Mendola JD. Abnormal sensory eye dominance in stereoanomalous subjects. *J Vis.* 2019;19(13):14.
20. Han C, He ZJ, Ooi TL. On sensory eye dominance revealed by binocular integrative and binocular competitive stimuli. *Invest Ophthalmol Vis Sci.* 2018;59(12):5140–5148.
21. Wang Y, He Z, Liang Y, et al. The binocular balance at high spatial frequencies as revealed by the binocular orientation combination task. *Front Hum Neurosci.* 2019;13:106.
22. Schor CM, Wood I. Disparity range for local stereopsis as a function of luminance spatial frequency. *Vision Res.* 1983;23(12):1649–1654.
23. Hess RF, Liu CH, Wang YZ. Luminance spatial scale and local stereo-sensitivity. *Vision Res.* 2002;42(3):331–342.
24. Tyler CW. Colour bit-stealing to enhance the luminance resolution of digital displays on a single pixel basis. *Spat Vis.* 1997;10(4):369–377.
25. Baldwin AS. alexsbaldwin/MatlabStaircase: v0.9.0. Zenodo, http://doi.org/10.5281/zenodo.3266142. Accessed July 2, 2019.
26. García-Pérez MA. Forced-choice staircases with fixed step sizes: asymptotic and small-sample properties. *Vision Res.* 1998;38(12):1861–1881.
27. Wilkinson F, Wilson HR, Habak C. Detection and recognition of radial frequency patterns. *Vision Res.* 1998;38(22):3555–3568.
28. Prins N, Kingdom FAA. Palamedes: Matlab routines for analyzing psychophysical data. www.palamedestoolbox.org; 2009.
29. Meese TS, Georgeson MA, Baker DH. Binocular contrast vision at and above threshold. *J Vis.* 2006;6(11):1224–1243.
30. Baker DH, Meese TS, Hess RF. Contrast masking in strabismic amblyopia: attenuation, noise, interocular suppression and binocular summation. *Vision Res.* 2008;48(15):1625–1640.

Investigative Ophthalmology & Visual Science